Research Article | Open Access

Soft Science

Cheng *et al. Soft Sci.* **2026**, *6*, 36 **DOI:**10.20517/ss.2025.123

Dual-function core-shell nanocube probes enabling continuous production of cortisol-sensing yarns via conjugate electrospinning

Jiang Cheng, Naihui Hou, Tengda Wang, Zhenyun Zhao*, Wei Chen*

Keywords:
Invasive cortisol sensing, dual-function core-shell NiHCF-MIP nanocubes, scalable conjugate electrospinning technique, flexible wearable sensing yarns

Citation: Cheng, J.; Hou, N.; Wang, T.; Zhao, Z.; Chen, W. Dual-function core-shell nanocube probes enabling continuous production of cortisol-sensing yarns via conjugate electrospinning. *Soft Sci.* **2026**, *6*, 36. https://dx.doi.org/10.20517/ss.2025.123

Received: 30 Nov 2025 **First Decision:** 26 Jan 2026 **Revised:** 21 Mar 2026 **Accepted:** 23 Apr 2026 **Published:** 13 May 2026

Academic Editor: Xinge Yu
Copy Editor: Xing-Yue Zhang
Production Editor: Xing-Yue Zhang

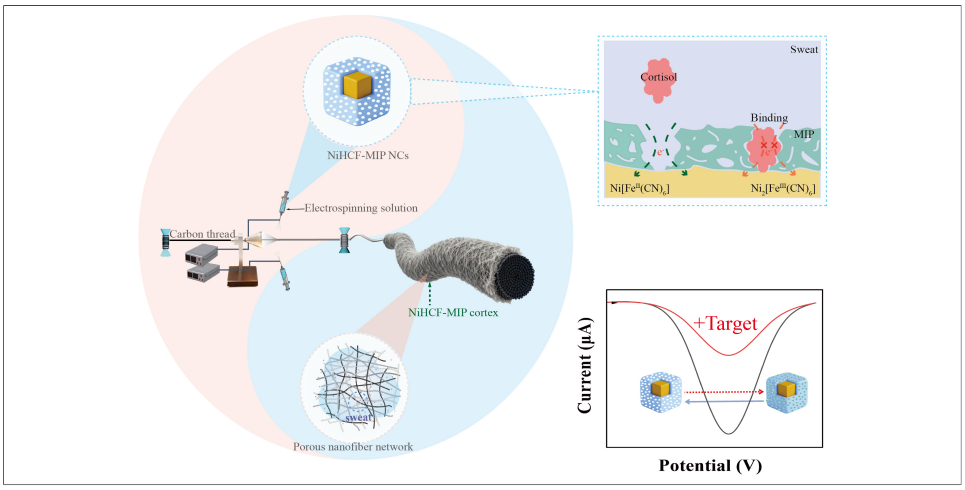

Abstract

With the growing global burden of chronic stress, there is an increasing need for real-time, non-invasive monitoring of cortisol dynamics. Molecularly imprinted polymer (MIP)-based sensing technology is known for its cost-effectiveness and low susceptibility to deactivation. Current invasive MIP-based cortisol sensors face fundamental requirements for improving sensitivity and widening the detection range. In addition, they encounter challenges in improving wearability and portability, as well as in developing commercially viable techniques. This work designs dual-function core-shell nickel hexacyanoferrate-MIP nanocubes (NiHCF-MIP NCs) and accordingly proposes a one-step conjugate electrospinning technique to yield coaxial cortisol-sensing yarns. The core-shell architecture effectively integrates the redox signal transduction capability of NiHCF with the cortisol-specific recognition function of MIP, enabling a continuous one-step fabrication process. The utilization of conjugate electrospinning technology not only supports scalable manufacturing but also creates a coaxial yarn structure that combines the advantages of the spun nanofiber network cortex and core threads. The as-produced yarns simultaneously possess high conductivity, flexibility, wearability, and rapid body fluid

National Engineering Lab for Textile Fiber Materials and Processing Technology, School of Materials Science and Engineering, Zhejiang Sci-Tech University, Hangzhou 310018, Zhejiang, China.

***Correspondence to:** Dr. Zhenyun Zhao, Prof. Wei Chen, National Engineering Lab for Textile Fiber Materials and Processing Technology, School of Materials Science and Engineering, Zhejiang Sci-Tech University, Hangzhou 310018, Zhejiang, China. E-mail: zhaozhenyun@zstu.edu.cn; wchen@zstu.edu.cn

absorption, collectively enhancing the sensing performance. Consequently, the electrospun yarns exhibit a high sensitivity of 2.08 μA·dec^{-1}, and the limit of detection (LOD) is theoretically calculated to be 0.4 nmol/L. This synergistic strategy combines core-shell dual-function nanomaterials with a one-step continuous conjugate electrospinning technique. It provides an innovative pathway for developing integrated wearable biosensing textiles for personal real-time stress monitoring and telehealth applications.

INTRODUCTION

Cortisol, a key glucocorticoid hormone[1], serves as a crucial biomarker for stress and overall homeostatic regulation[2]. The increasing global burden of chronic stress highlights the urgent necessity for continuous monitoring of cortisol dynamics[3]. Traditional cortisol assessment mainly depends on invasive blood sampling, which is inadequate for capturing the fluctuations of cortisol secretion or for achieving long-term and patient-centered monitoring[4]. Sweat, as a non-invasively accessible biofluid, has attracted substantial attention as an alternative analyte for cortisol detection[5,6].

Various recognition strategies have been explored for cortisol sensors in sweat analysis, such as antibodies, DNA aptamers[7,8], and molecularly imprinted polymers (MIPs)[9]. Cortisol-antibodies and cortisol-DNA aptamers usually suffer from high production costs, susceptibility to denaturation, and limited shelf-life. MIPs feature molecular-scale cavities that exhibit spatial and chemical complementarity to target analytes, thereby conferring lock-and-key specificity. This specificity has led to their designation as synthetic antibodies[10]. Their densely cross-linked polymeric structure imparts high physicochemical robustness, enabling stability under extreme pH, in organic solvents, at elevated temperatures, and under high pressure. The fabrication process involves a single-step copolymerization of functional monomers, cross-linkers, and template molecules, thereby eliminating the need for animal immunization or cell culture, while offering considerable cost advantages over biological antibodies and DNA aptamers. The fabrication process relies on a single-step copolymerization of functional monomers, cross-linkers, and template molecules. Therefore, it eliminates the need for animal immunization or cell culture. Moreover, this approach offers considerable cost advantages over biological antibodies and DNA aptamers.

Early MIP-based electrochemical sensors required external, solution-phase redox probes for signal transduction, such as adding the ferricyanide/ferrocyanide couple into electrolyte solutions[11]. This reliance confined their use to laboratory conditions, precluding their applications in continuous monitoring. A pivotal advancement involved integrating a stable internal transducer with the molecularly imprinted polymer (MIP). Typical examples include Prussian blue (iron hexacyanoferrate, FeHCF) and its analogues, such as nickel, copper, and cobalt hexacyanoferrates (named NiHCF, CuHCF, and CoHCF, respectively). These materials contain the ferricyanide/ferrocyanide redox couple[12,13].

In this architecture, MIPs are subsequently deposited onto Prussian blue (or its analogues) layers[14]. For example, in 2021, Wang et al. pioneered flexible and wearable electrochemical patch-type sensors by screen-printing Prussian blue slurry onto stretchable Perme-Roll Lite films and then electrodepositing cortisol-MIP[15]. The flexible patch-type sensors can monitor cortisol secretion in fingertip sweat. The limit of detection (LOD) is 0.9 nmol/L, and the sensitivity is 38.8 nA·dec^{-1}. This breakthrough has enabled continuous laboratory-free detection of biofluids. High-resolution patterning techniques, such as screen printing, intaglio transfer printing[16], and inkjet printing, offer distinct fabrication pathways for biosensors.

Even so, a key challenge remains in developing truly comfortable, soft, large-scale wearable MIP-based sweat cortisol sensors. Existing types are mainly presented as patch-type devices[17], which can cause discomfort, hinder natural skin breathability, and exhibit poor long-term adhesion. To overcome these limitations, there

is a clear demand for sensors that are able to seamlessly integrate into daily textiles. Currently, there are only a few reports on cortisol-sensing textiles[18], and their technological routes mainly include conventional coating as well as chemical and electrochemical deposition[19]. On the one hand, they significantly compromise the inherent advantages of textiles, including softness, conformability to skin, and moisture absorption. This greatly diminishes comfort and long-term wearability. On the other hand, the reported preparation routes are multi-step and discontinuous, typically including the preparation of conductive textile substrates followed by the deposition of functional layers in sequence.

Herein, we designed dual-function core-shell nickel hexacyanoferrate-MIP (NiHCF-MIP) nanomaterials and presented a scalable continuous conjugate electrospinning technology. Using this approach, we obtained coaxial sensing yarns that are capable of real-time monitoring of sweat cortisol. The coaxial yarn shows high specificity to cortisol, a high sensitivity of 2.08 μA·dec^{-1}, and a low LOD of 0.4 nmol/L. The dual-function core-shell NiHCF-MIP NCs integrate redox-probing cores with cortisol-recognizing shells, which is beneficial for signal transport and also enables one-step continuous production [Figure 1A]. In addition, the coaxial configuration produced by conjugate electrospinning[20,21], with conductive yarns as the core and cortisol-sensing nanofibers as the cortex, combines conductivity, flexibility, and sensing capability[22]. Furthermore, the porous morphology of the nanofiber cortex enhances sweat absorption and interfacial contact [Figure 1B]. This work will facilitate the construction of a wearable biosensing platform for personalized stress and health assessments [Figure 1C], as well as provide a commercially viable technical methodology.

EXPERIMENTAL

Reagents and materials

Ferrous acetate ($Fe(CH_3COO)_2$), nickel(II) acetate tetrahydrate ($Ni(CH_3COO)_2·4H_2O$), trisodium citrate dihydrate ($Na_3Cit·2H_2O$), potassium ferricyanide ($K_3[Fe(CN)_6]$), acetic acid, cortisol, pyrrole (Py), methanol, urea, ethylene glycol dimethacrylate (EGDMA), 2,2-azobis(isobutyronitrile) (AIBN), ascorbic acid (AA), phosphate-buffered saline (PBS), Artificial sweat, and N, N-dimethylformamide (DMF) were purchased from Macklin Co., Ltd. (Shanghai, China). Polyacrylonitrile (PAN, Mw 85,000), poloxamer (F127), Progesterone, cortisone, prednisolone, corticosterone, creatinine, and multiwall carbon nanotubes (MWCNTs, OD: 8-15 nm, length: 50 μm) were purchased from Aladdin Co., Ltd. (Shanghai, China). Thermoplastic polyurethane (TPU) was provided by BASF Co., Ltd. (Shanghai, China). Conductive carbon threads were from Taobao.

Preparation of NiHCF NCs

The redox probe nanomaterial prepared herein is a type of Prussian blue analogue, specifically nickel hexacyanoferrate nanocubes (NiHCF NCs). A modified low-temperature coprecipitation reaction method was proposed[23]. At first, 600 μmol of $Fe(CH_3COO)_2$ and 900 μmol of $Na_3Cit·2H_2O$ were dissolved in 20 mL of deionized water to form solution A, while 400 μmol of $K_3[Fe(CN)_6]$ was dissolved in another 20 mL of deionized water to prepare solution B. Solution A was then added dropwise to solution B at a flow rate of 20 mL/min under continuous stirring at 1,000 r/min, followed by a coprecipitation reaction at a low temperature of 5 °C for 24 h. The resulting precipitate was collected by centrifugation at 11,000 r/min for 10 min. The pellet was washed four times with 60 mL of deionized water. Finally, the purified product was dried in a vacuum oven at 40 °C for 12 h to obtain NiHCF NCs.

Preparation of dual-function core-shell NiHCF-MIP NCs

The core-shell NiHCF-MIP NCs were prepared via thermally initiated free radical copolymerization[24], employing pyrrole as the functional monomer and EGDMA as the cross-linker, to construct a molecularly imprinted polymer (MIP) network, followed by a cortisol elution process [Figure 1A]. Pyrrole primarily

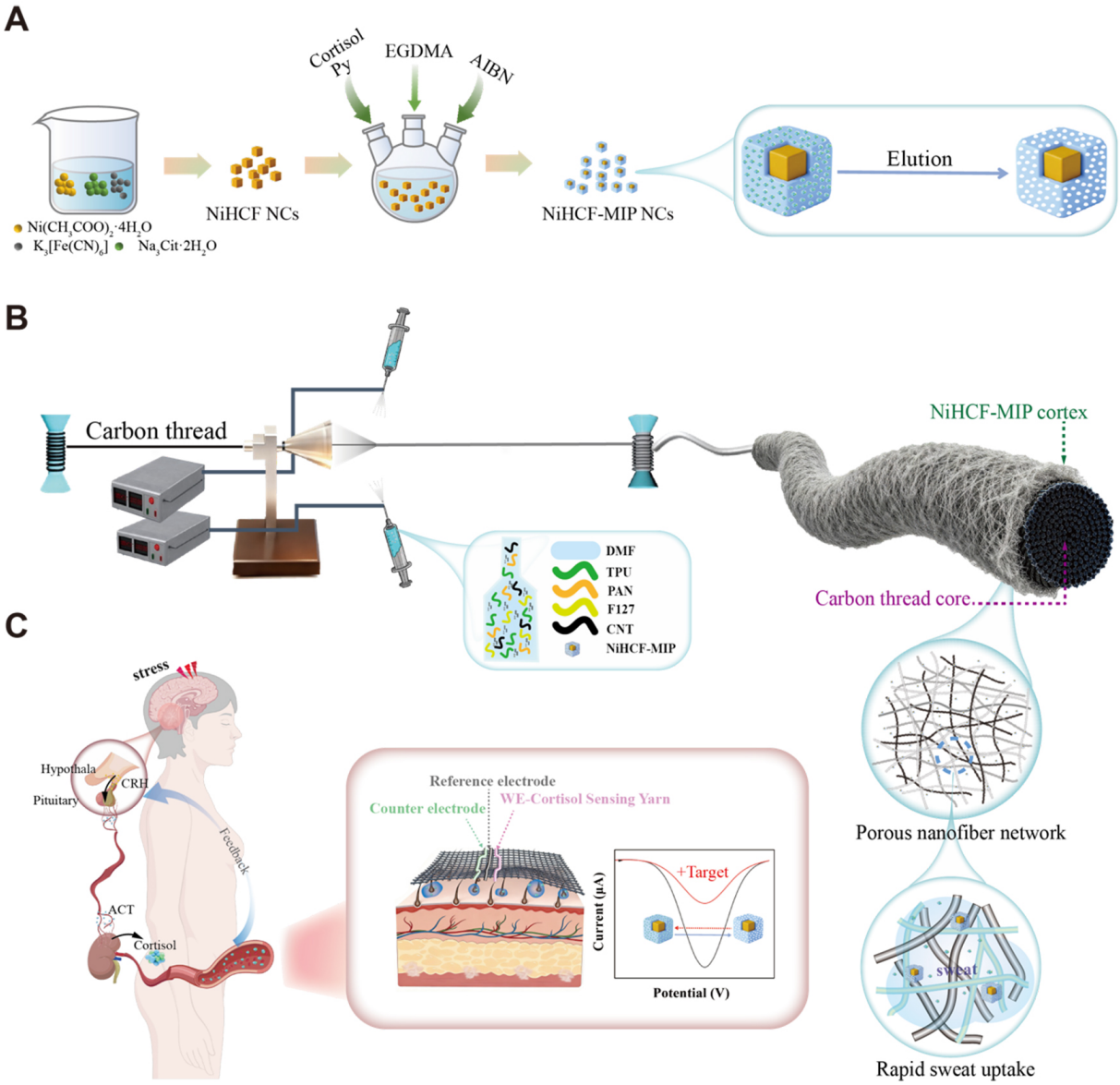

Figure 1. (A) Preparation of dual-function core-shell NiHCF-MIP NCs; (B) One-step continuous conjugate electrospinning technique to wrap NiHCF-MIP NCs nanofibers around conductive carbon thread; (C) Scheme of secretion process and stress management mechanism of cortisol, along with real-time stress-monitoring demonstration of wearable textile sensors prepared with the proposed sensing yarns. The pattern was created with BioGDP.com. NiHCF: Nickel hexacyanoferrate; MIP: molecularly imprinted polymer; NCs: nanocubes; Py: pyrrole; EGDMA: ethylene glycol dimethacrylate; AIBN: 2,2-azobis(isobutyronitrile); DMF: dimethylformamide; TPU: thermoplastic polyurethane; PAN: polyacrylonitrile; CNT: carbon nanotube; CRH: corticotropin-releasing hormone; ACT: adrenocorticotropic hormone; WE: working electrode.

provides hydrogen-bonding recognition sites for the template molecule and copolymerizes with EGDMA under AIBN initiation to form a highly cross-linked, non-conductive imprinted polymer. The samples before and after cortisol elution are referred to as NiHCF-MIP (BE) and NiHCF-MIP (AE), respectively, and the only difference between them is the presence or absence of cortisol-imprinted cavities.

The polymerization system consisted of the target molecule (cortisol), monomer (pyrrole), crosslinking agent (EGDMA), and initiator (AIBN). Specifically, 8 mM of cortisol, 20 mM of Py, 40 mM of EGDMA, and 15 mg of NiHCF NCs powder were homogeneously dispersed in 10 mL of a deionized water/methanol mixture (volume ratio 1:4). The solution was subjected to three cycles of degassing (vacuum evacuation followed by

nitrogen purging) to eliminate dissolved oxygen. Subsequently, the mixture was stirred at 500 r/min for 24 h at 25 °C. Then, 25 mM of AIBN was added, and another three cycles of degassing were performed to maintain an inert atmosphere and prevent side oxidations, particularly decarboxylation. The reaction vessel was then placed in a 40 °C water bath and continuously stirred at 500 r/min for 5 h to initiate radical polymerization and form the polypyrrole shell on the NiHCF nanocube core, obtaining the NiHCF-MIP (BE) sample. In addition, a non-imprinted polypyrrole (NIP) shell-coated sample (NiHCF-NIP NCs) was also prepared for contrast. This sample was synthesized without the addition of cortisol molecules during polymerization.

After polymerization, the centrifugation-collected product was immersed in 5 mL of an acetic acid/methanol mixture (volume ratio 7:3), followed by stirring at 500 r/min for 12 h to effectively remove the target molecule and generate the cortisol molecular imprinting cavities. The extracted material was washed with deionized water three times and with methanol once. Finally, the purified core-shell NiHCF-MIP NCs were dried under vacuum at 30 °C for 12 h, yielding the cortisol-sensing material. In the following text, unless otherwise stated, NiHCF-MIP denotes samples that have undergone the elution process and possess cortisol cavities.

Preparation of carbon cloth coated with NiHCF-MIP NCs

To preliminarily evaluate the sensing performance of NiHCF-MIP NCs, 5 mg of NiHCF-MIP NCs were dissolved in 3 mL of anhydrous ethanol and ultrasonicated for 5 minutes to achieve uniform dispersion. Next, 50 μL of the dispersion was drop-cast onto a 1 cm × 1 cm commercial carbon cloth and allowed to dry. This drop-casting procedure was repeated three times. The prepared carbon cloth was employed as the working electrode for electrochemical testing in a threeelectrode system.

Preparation of spinning solution

The spinning solution consists of DMF as the solvent, PAN and TPU as hydrophilic thermoplastic polymers, poloxamer F127 as a dispersing agent, MWCNTs as a conductive additive[25], and core-shell NiHCF-MIP NCs as the cortisol-sensing active material. These solid components (NiHCF-MIP NCs, MWCNTs, PAN, TPU, and F127) are in a mass ratio of (3-12):10:300:100:100. The total solid mass to DMF volume ratio ranges from 5.13 to 5.22 g per 20 mL.

To prepare the solution, PAN, F127, and TPU were first dissolved in DMF under continuous stirring at 40 °C for 2 h, yielding a colorless, transparent, and viscous solution. MWCNTs were then introduced into this solution and stirred at 40 °C for an additional 2 h. Next, NiHCF-MIP NCs were added and stirred at the same temperature for 1 h to achieve uniform distribution throughout the polymer matrix. Finally, the mixture was ultrasonicated at 300 W for 1 h to remove entrapped air bubbles, yielding a stable and homogeneous spinning solution.

Preparation of coaxial cortisol-sensing yarns

The cortisol-sensing yarn was fabricated via conjugate electrospinning. In this process, a conductive carbon thread was positioned at the center as the core yarn. A nanofiber layer consisting of NiHCF-MIP NCs was wrapped around the conductive carbon thread to form a coaxial structure [Figure 1B]. A 5 mL syringe equipped with a 20 G needle was used. The two spinnerets were set to voltages of +12.5 and -12.5 kV, respectively, and were aligned 15 cm apart, directly facing the center of the rotating collecting horn at a distance of 10 cm. During conjugate electrospinning, the micro-pump feeding rate was maintained at 1-3 mL/h, the collecting horn rotated at 100-200 r/min, the diameter of the take-up roll was 4.78 cm, and its rotational speed was 0.8 r/min. The production rate per hour is calculated using Equation 1:

$$\text{Production Rate (m/h)} = (\pi d) \times \omega \times 60 \quad (1)$$

Here, d represents the diameter of the take-up roll, and ω represents the rotational speed. Therefore, the cortisol-sensing yarn collection speed is 7.2 m/h. The process was carried out under a temperature of 30 ± 5 °C and a relative humidity of 50% ± 10%. The same conductive carbon thread was repeatedly subjected to this conjugate electrospinning process for 1 to 4 cycles to achieve a well-defined coaxially structured cortisol-sensing yarn.

Characterization and measurement

The surface and cross-section morphologies, as well as elemental compositions, were analyzed using field emission scanning electron microscopy coupled with energy dispersive spectroscopy (FESEM-EDS, Gemini500). The fine microstructure of NiHCF-MIP NCs was examined by high-resolution transmission electron microscopy (HRTEM, Thermo Fisher Scientific Talos F200X G2). Chemical composition and crystal structure were characterized by Fourier transform infrared spectroscopy (FTIR, Nicolet 5700) and X-ray diffraction (XRD, Bruker D8 A8 Advance), respectively. Electrochemical performance was assessed using a standard three-electrode system and an electrochemical workstation (CHI760E). The cortisol-sensing yarn served as the working electrode, an Ag/AgCl electrode as the reference electrode, and a platinum sheet as the counter electrode. The electrolyte was 0.1 M phosphate-buffered saline (PBS, pH 6.5) with cortisol concentrations ranging from 100 to 10^5 nmol/L. The sensing parameters (including sensitivity, limit of detection (LOD), incubation time, detection range, coefficient of determination (R^2)) were determined from linear sweep voltammetry (LSV) curves recorded within a potential window of 0.6 to -0.2 V at a scan rate of 10 mV/s[26].

Calculation method

Sensitivity (s) and LOD were calculated according to IUPAC recommendations[27]. A logarithmic linear fitting of current differences (ΔI, μA) *vs.* cortisol concentrations $\log_{10}$([cortisol] (nmol/L)) was first performed. Sensitivity was obtained from the slopes of linear fitting plots. LOD was calculated by multiplying the average standard deviation (σ) by 3 and dividing by the sensitivity (s), as follows (see Equation 2),

$$LOD = 3\sigma / s \quad (2)$$

RESULTS AND DISCUSSION

Structures of core-shell NiHCF-MIP NCs

NiHCF acts as a crucial internal redox probe, transmitting electrochemical signal differences caused by cortisol molecules. The SEM image of NiHCF [Figure 2A] confirms its uniform nanocube shape with a size of ~100 nm. Based on the nanocube templates, MIP is *in situ* chemically grown on their surface, and the SEM image of NiHCF-MIP is shown in Figure 2B. The *in situ* growth of MIP does not cause significant shape changes or size expansion, and the uniform nanocube structure with a size of ~100 nm is still clearly observed in the TEM image of NiHCF-MIP [Figure 2C]. Further, HRTEM and EDXS are recorded to characterize its fine micro-architecture and elemental distribution [Figure 2D and E]. NiHCF-MIP shows a unique core-shell nanocube structure; Fe, Ni, and O elements mainly distribute at the core part, and C and N distribute around both core and shell parts. NiHCF contains a large quantity of Fe and Ni elements, and MIP is mainly composed of C and N elements. Thus, the core-shell structure, with NiHCF as the core and MIP as the shell, is confirmed. Furthermore, the intimately bonded interface between the NiHCF core and MIP shell [Figure 2F] indicates their close integration. This way, once the cavities in the MIP shell are filled by cortisol molecules, the resultant electrochemical signal changes can be instantly captured by the internal probing NiHCF core. On the one hand, the core-shell structural design of NiHCF-MIP NCs can increase response speed; on the other hand, the dual-function nature enables one-step, continuous production routes, avoiding conventional separate step-by-step deposition of redox-probing and cortisol-sensing layers.

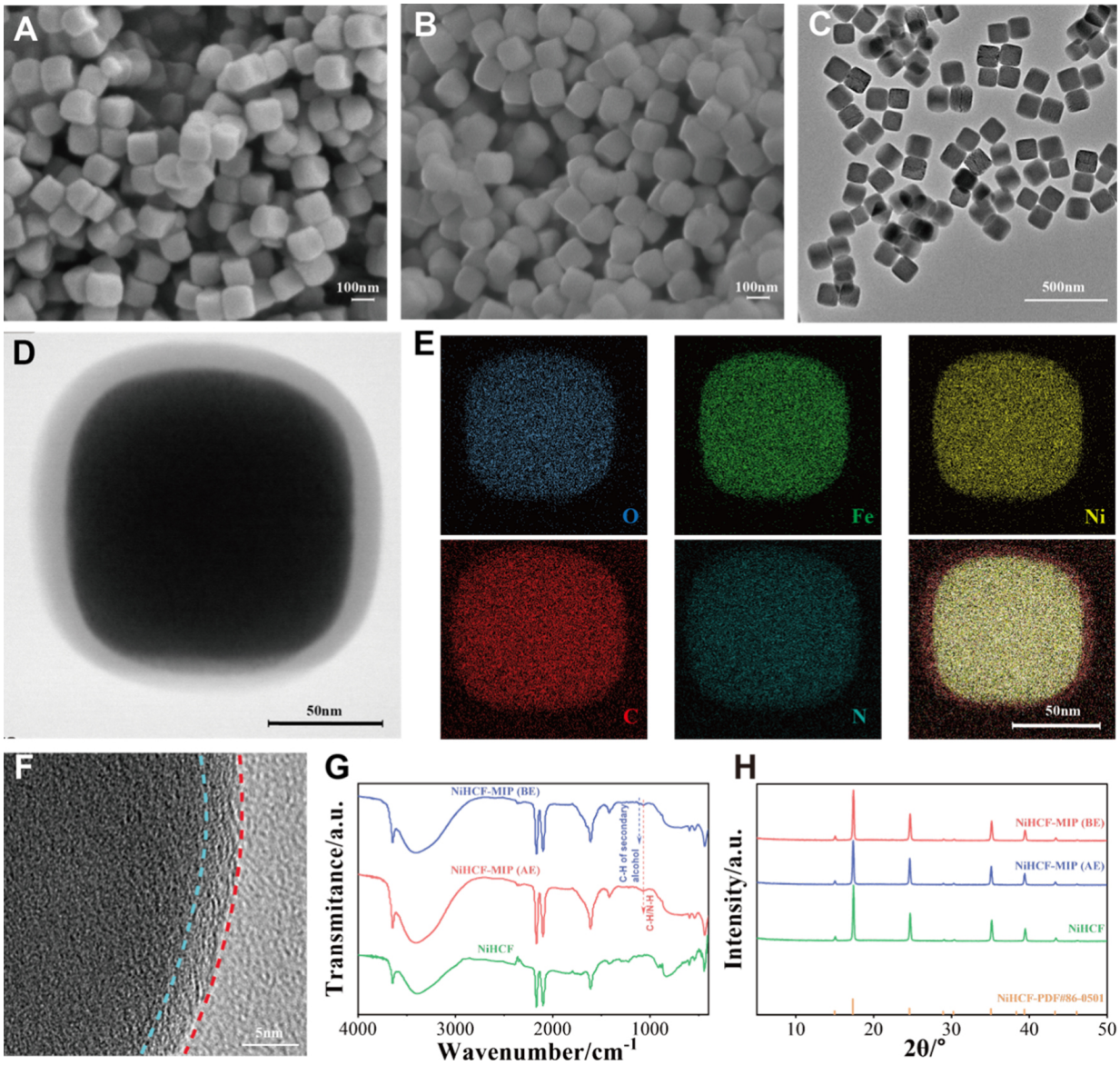

Figure 2. (A and B) Morphologies of NiHCF and NiHCF-MIP NCs; (C) TEM image of NiHCF-MIP NCs; (D and E) HRTEM image of the core-shell microstructure of one NiHCF-MIP nanocube and its EDXS mapping; (F) HRTEM image of the interface between the NiHCF core and the MIP shell; (G) FTIR and (H) XRD curves of NiHCF, NiHCF-MIP (BE), and NiHCF-MIP (AE) samples. NiHCF: Nickel hexacyanoferrate; MIP: molecularly imprinted polymer; NCs: nanocubes; TEM: transmission electron microscopy; HRTEM: high-resolution transmission electron microscopy; EDXS: energy-dispersive X-ray spectroscopy; FTIR: Fourier-transform infrared spectroscopy; XRD: X-ray diffraction; BE: before elution; AE: after elution; PDF: Powder Diffraction File.

Chemical compositions and crystal structures of NiHCF, NiHCF-MIP (BE), and NiHCF-MIP (AE) samples are characterized by FTIR and XRD technologies. Their characteristic peaks in FTIR are generally similar, except for the emergence of a new peak at 1,065 cm^{-1} in the NiHCF-MIP (BE) and NiHCF-MIP (AE) samples, which corresponds to the in-plane deformations of C-H and N-H from polypyrrole[28], confirming the fabrication of a polypyrrole shell [Figure 2G]. Both NiHCF-MIP(BE) and NiHCF-MIP(AE) display characteristic absorption bands at 1,707 and 1,204 cm^{-1}, respectively, assigned to steroid C-O and C-O-C stretching vibrations, along with a 1,437 cm^{-1} feature arising from methylene C-H bending vibrations[29]. These spectral features collectively originate from cortisol and the EGDMA cross-linker incorporated during

the imprinting process. When the FTIR spectra of NiHCF-MIP (BE) and NiHCF-MIP (AE) are compared, a weak peak at ~1,118 cm^{-1} is observed in the BE sample. This peak, assigned to the C-H bond of secondary alcohol structures, disappears after the cortisol-elution process[30]. Their XRD peaks [Figure 2H] correspond well to PDF#86-0501, which has the chemical formula of $Ni[Fe(CN_6)]_{0.667}{\cdot}H_2O_{3.333}$ with a cubic phase (F43m space group), characterized by the unit cell parameter of 10.23 Å × 10.23 Å × 10.23 Å. The main diffraction peaks at 17.3°, 24.6°, 35.1°, and 39.4° are assigned to (200), (220), (400), and (420) planes, respectively. Their peak positions and intensities are almost identical, indicating that the deposition of polypyrrole and the elution of cortisol did not adversely affect the crystal structures. This ensures high stability during subsequent processing, electrochemical measurements, and long-term practical use.

Structures and characteristics of conjugate electrospun yarns

Conjugate electrospinning technology is a promising method for the scalable and cost-effective fabrication of biosensors. This technology enables one-step, continuous, large-scale fabrication of a 'conductive core-sensing cortex' structure. In this structure, the conductive carbon core and the sensing nanofiber cortex work synergistically to reduce charge-transfer resistance and enhance the current response of the yarn-type sensor[31]. This technology also synergistically enhances the interaction between the nanoparticles and the electrospun nanofiber network. The small-sized sensing particles and electrospun nanofiber network construct a high-surface-area architecture. This architecture increases the density of specific recognition sites and enhances fiber surface hydrophilicity. Consequently, it promotes rapid sweat absorption. This technology produces a cortisol-sensing yarn that is conductive, flexible, hydrophilic, and sensitive to cortisol. Thus, the conjugate electrospinning technology was selected, which applies oppositely charged nozzles and a trumpet-like rotating collector to electrospin nanofiber networks onto the core yarn, winding and twisting[32]. Herein, the electrically conductive and mechanically flexible carbon threads are utilized as the core part; the cortisol-sensing NiHCF-MIP NCs are electrospun to form a nanofiber-network cortex with the assistance of a hydrophilic polymer matrix [Figure 3A]. This technology enables continuous preparation of cortisol-sensing yarns at a rate of 7.2 m/h [Figure 3B].

The surface morphology of the NiHCF-MIP cortex is shown in Figure 3C and D, from which nanofiber networks together with nanoporous microstructure can be observed. In addition, a coaxial structure with the conductive carbon thread and NiHCF-MIP nanofiber as core and cortex parts is demonstrated in the yarn cross-section [Figure 3E]. Elemental surface mapping is shown in Figure 3F and Supplementary Figure 1, from which a large number of Fe, Ni, C, N, and O elements are detected, indicating encapsulation of the NiHCF-MIP nanofiber network around the core carbon thread.

Fast sweat absorption ability is crucial for sweat-sensing yarns. Herein, we used a type of aqueous fluorescent dye to demonstrate the rapid water absorption process of this sensing yarn [Figure 3G and Supplementary Movie 1]. We aspirated 10 μL of fluorescent dye using a pipette and dropped it onto the cortex of the sensor yarn. Due to the hydrophilic groups and nanoporous structure of the sensing cortex, once 10 μL of aqueous fluorescent dye was applied to the yarn, it completely permeated 3 cm of the sensor yarn within 5 seconds. To further test the hydrophilicity of the nanofiber cortex, an electrospun nanofiber film from the spinning solution was collected for WCA measurement. The WCAs were recorded by a high-speed camera [Figure 3H and Supplementary Movie 2]. The measured WCAs were 32.55° after 33 ms and 8.52° after 100 ms, respectively, and the water droplet was completely absorbed after 133 ms. Liquid absorption ability is mainly related to surface chemistry and physical structures. The spinning solution contains large amounts of PAN and F127, which are rich in -C≡N and ethylene/propylene oxide structures. Furthermore, the conjugate electrospun cortex features a nanofiber network-like and micro/nanoporous morphology, which greatly enhances hydrophilicity and ensures rapid sweat absorption. The Young-Laplace equation (see Eqation 3) was used to quantitatively characterize the transport and distribution dynamics of sweat within the porous epidermal layer of cortisol-sensing yarns:

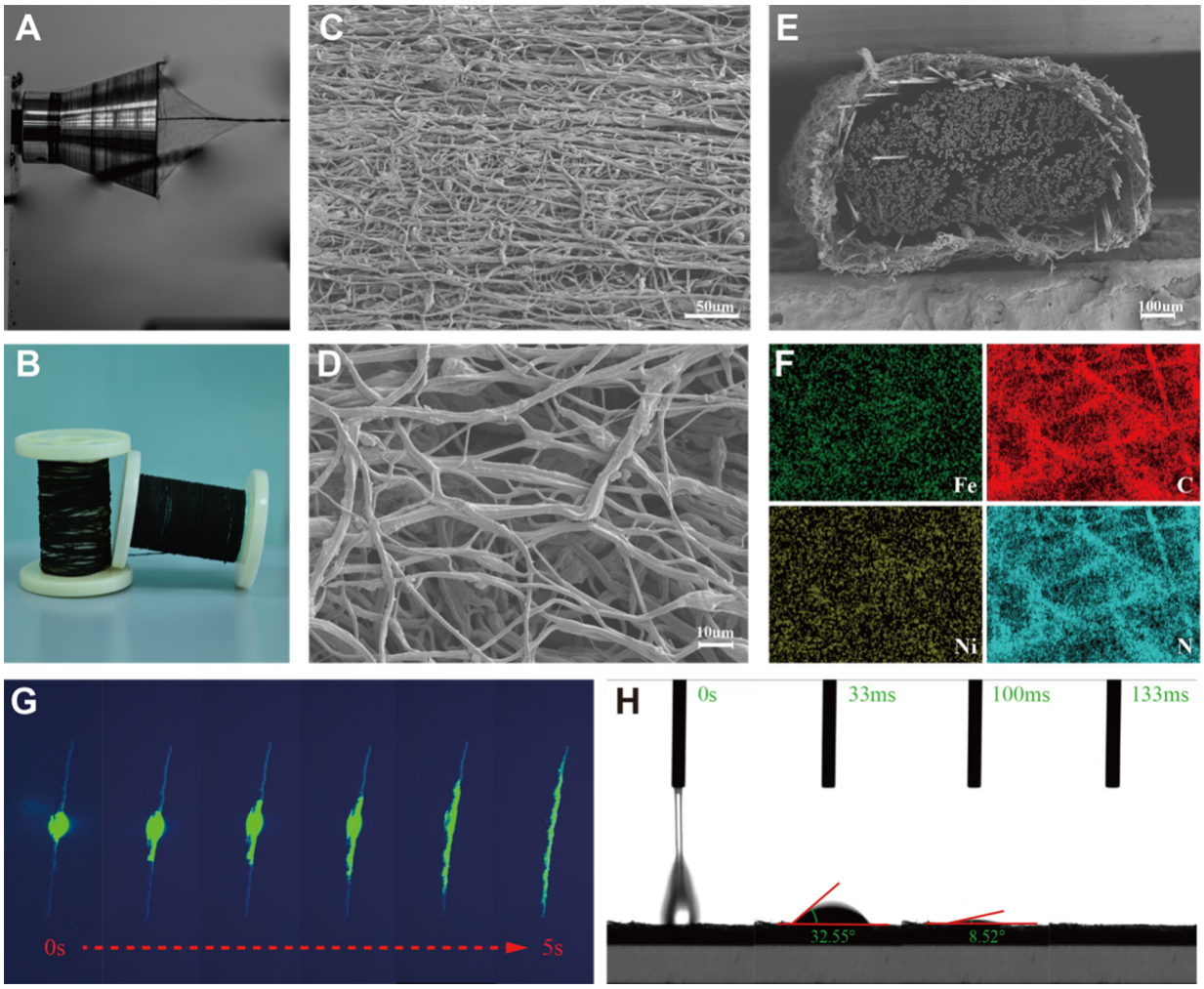

Figure 3. (A) Photo of conjugate electrospinning preparation of cortisol-sensing yarns; (B) Two rolls of cortisol-sensing yarns prepared through continuous conjugate electrospinning technology; (C and D) Surface morphology of cortisol-sensing yarns under low and high magnification; (E) Cross-section SEM image and (F) surface elemental mapping of a cortisol-sensing yarn; (G) Photos of dye infiltration into a cortisol-sensing yarn within 5 s; (H) WCA of electrospun sensing films within 133 ms. SEM: Scanning electron microscopy; WCA: water contact angle.

$$P = 2\gamma \cos\theta / r \quad (3)$$

Here, P denotes the Laplace pressure, corresponding to the capillary force (F_c); γ represents the surface tension of the liquid; θ signifies the instantaneous contact angle; and r indicates the mean pore radius between fibers. This capillary force (F_c) originates from the surface energy gradient established between sweat and the nanoscale pores of the sensing cortex, while the permeable nanoporous structure significantly enhances this capillary effect, thereby accelerating the capillary dynamics of sweat. Upon initial contact, sweat is rapidly drawn into the nanofiber network through the synergistic action of capillary force (F_c) and omnidirectional wetting forces (F_w). Subsequently, sweat is adsorbed onto adjacent fibers and within interstitial pores, leading to rapid spreading and permeation throughout the yarn cortex.

In real-world wearable applications, an excellent sweat absorption ability will definitely shorten the collection time and incubation time of sweat samples, contributing to real-time monitoring of cortisol concentration levels. Besides, the porous nanofiber network morphology creates a large interfacial contact area, conducive to binding cortisol molecules and enhancing signal differences and sensitivities.

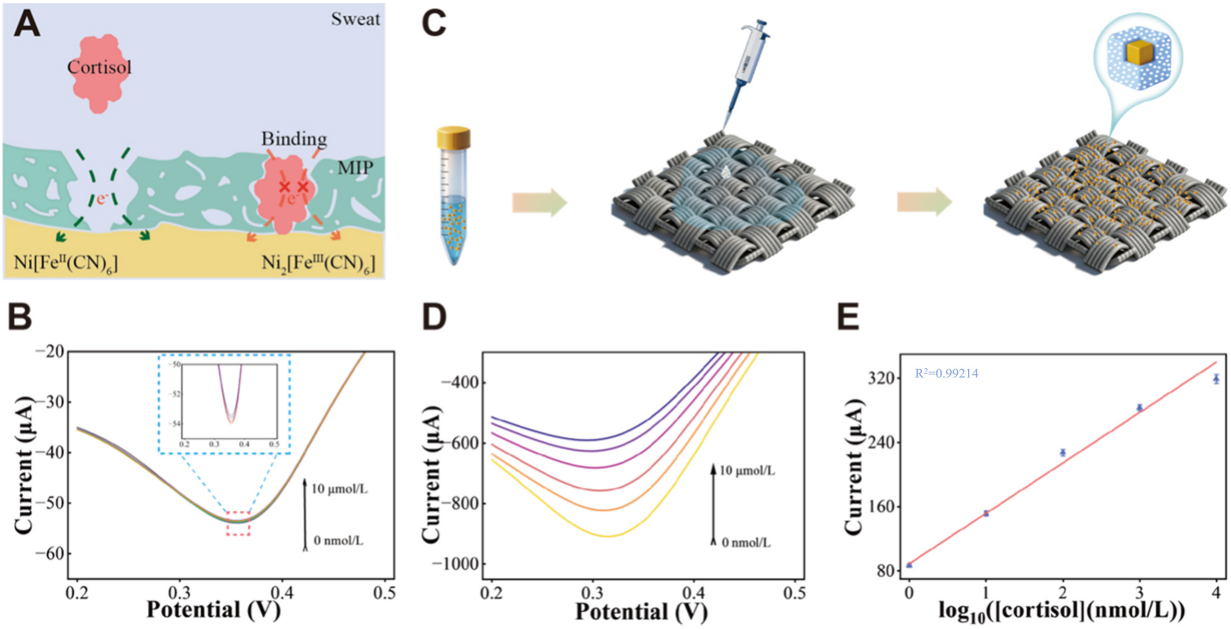

Figure 4. (A) Sensing mechanism of NiHCF-MIP NCs; (B) LSV curves of NiHCF-NIP-prepared yarns; (C) Preparation of carbon cloth coated with NiHCF-MIP NCs; (D) LSV curves and (E) linear-fitting data of the commercial carbon cloth prepared by drop-casting NiHCF-MIP NCs dispersion, and tested in blank and 1 nmol/L~10 μmol/L cortisol (n = 3, signifying 3 independent sensors). Error bars represent the SD of the mean from three sensors in (E). NiHCF: Nickel hexacyanoferrate; MIP: molecularly imprinted polymer; NCs: nanocubes; LSV: linear sweep voltammetry; SD: standard deviation.

Cortisol-sensing properties

MIP shells were *in situ* formed onto NiHCF NC cores after pre-absorption and thermal polymerization processes; subsequent elution of cortisol yields cortisol-selective cavities within MIP shells. In this way, the core-shell NiHCF-MIP NCs are able to selectively recognize cortisol molecules. The sensing mechanism is based on the selective binding of cortisol to the cavities in the MIP shell. This binding impedes charge transfer to the embedded NiHCF redox probe[33], thereby reducing the electrochemical signal intensity. The signal reduction can be quantified by LSV (see the Experimental section for more calculation details) [Figure 4A]. NIP shells lack cortisol-selective cavities, so the NiHCF-NIP NCs hardly exhibit signal changes before and after the addition of cortisol [Figure 4B].

Currently, the functionalization of molecularly imprinted sweat sensors primarily relies on *in situ* electrodeposition. This method involves sequential deposition of electrochemical signal probes and molecularly imprinted layers onto the surface of conductive substrates, a process that is laborious and difficult to adapt to large-scale continuous production. Unlike previous studies, we have designed and fabricated bifunctional core-shell NiHCF-MIP NCs that integrate both target recognition and signal transduction functions, offering high scalability. Here, the cortisol-sensing performance of the bifunctional core-shell NiHCF-MIP NCs coated on commercial carbon cloth was validated. Briefly, 5 mg of NiHCF-MIP NCs were dispersed in 3 mL of anhydrous ethanol, and 50 μL aliquots of the resulting suspension were uniformly drop-casting onto 1 cm × 1 cm commercial carbon cloth substrates, followed by drying. This coating process was repeated three times [Figure 4C]. The LSV responses and corresponding linear fitting data are presented in Figure 4D and E. A high sensitivity of 46.44 μA·dec^{-1} (tested on a commercial carbon cloth substrate) is achieved over a detection range of 1 nmol/L to 10 μmol/L for cortisol, together with a high R^2 over 0.992, confirming the excellent cortisol-sensing performance of NiHCF-MIP NCs. This is primarily attributed to their unique core-shell structure design that effectively integrates the redox-probing core with the cortisol-sensing shell, enabling simultaneous signal transduction and selective molecular recognition.

Thus, electrochemical signal changes can be instantly captured by the NiHCF core upon specific binding of cortisol to the MIP shell. Furthermore, such dual-function core-shell NiHCF-MIP NCs are compatible with various continuous and scalable fabrication techniques[34], including drop coating, spray coating, spin coating, printing, and spinning. Herein, we selected the conjugate electrospinning technique, primarily for obtaining better wearability, comfort, sweat-absorption ability, and seamless integration into textile-based biosensing platforms.

Processing parameters of conjugate electrospinning technology have a significant influence on the cortisol-sensing properties of yarns. Repeating cycles of the conjugate electrospinning process were first systematically selected through electrochemical impedance spectra (EIS). EIS for 2, 4, and 6 electrospinning cycles were tested [Supplementary Figure 2], all showing a semi-circle followed by an oblique line, indicative of charge transfer resistance and electrolytic diffusion ability. As shown in Supplementary Figure 2, the yarn subjected to four electrospinning cycles exhibits a smaller semicircle in the Nyquist plot, indicating that charge transfer occurs more easily at the electrode-electrolyte interface, which corresponds to a lower charge transfer impedance. Additionally, the sloped region observed at low frequencies in the Nyquist plot originates from diffusion-controlled mass transport and is conventionally referred to as Warburg impedance. The Nyquist plot of the yarns subjected to four electrospinning cycles demonstrates the steepest low-frequency slope, indicating the minimal Warburg impedance and the fastest ion diffusion. This is because increasing repetition can thicken the NiHCF-MIP nanofiber cortex, which increases the number of cortisol-selective cavities but conversely elongates the electronic transport distance between the superficial sensing layer and centered conductive yarn. Accordingly, an optimal repeating cycle of four was selected for further investigation. Given the inherent pH fluctuations in sweat, we initially evaluated the LSV response of the sensor to a fixed cortisol concentration (1 μmol/L) in PBS buffers at different pH values [Supplementary Figure 3]. The data indicate that the sensor achieved the maximum response current at pH 6.5. Consequently, all subsequent experiments were conducted in PBS at pH 6.5.

Another factor is the amount of NiHCF-MIP NCs in the spinning solution. Weight ratios of NiHCF-MIP NCs to total solid components at 0.6, 1.2, and 2.4 wt% were tested. Their LSV responses [Figure 5A-C], linear fitting curves [Figure 5D], and current difference and sensitivity data [Figure 5E] were used to evaluate the cortisol-sensing properties. All LSV tests were conducted after a short incubation time of 120 s with a scan rate set as high as 0.01 V/s. All samples demonstrated high R^2 values exceeding 0.95 in a wide detection range of 1 nmol/L to 10 μmol/L for cortisol molecules. In comparison, higher amounts of NiHCF-MIP NCs provide more cortisol-selective cavities and thus improve sensing performance. Specifically, a content of 2.4 wt% achieves a high sensitivity of 2.08 μA·dec^{-1} with an R^2 value of 0.994, and its calculated LOD is as low as 0.4 nmol/L [see Equation (1)]. Compared to previous related reports, our coaxial yarns show significant advantages in sensitivity, LOD, and incubation time [Table 1]. The dual-function core-shell NiHCF-MIP NCs, coaxial yarn configuration, strong sweat-absorption ability, and porous morphology of nanofiber cortex layers are all contributors to the excellent cortisol-sensing properties. To evaluate the performance of the NiHCF-MIP fiber sensor in a more complex environment, tests were conducted using artificial sweat containing varying concentrations of cortisol. As the cortisol concentration in the artificial sweat increased, a notable decrease in the LSV peak current was observed [Figure 5F], demonstrating a linear relationship between the logarithm of the peak current difference and cortisol concentration on a logarithmic scale, with a sensitivity of 1.15 μA·dec^{-1} and R^2 values exceeding 0.99.

Furthermore, the MIP sensing layer affords ultrahigh selectivity by virtue of specific hydrogen-bonding recognition sites and cortisol-complementary imprinted cavities that discriminate target molecules from structurally analogous interferents. As demonstrated in Figure 5G, when common sweat constituents, including glucose (Glu), lactate (Lac), uric acid (UA), tryptophan (Try), ascorbic acid (AA), progesterone,

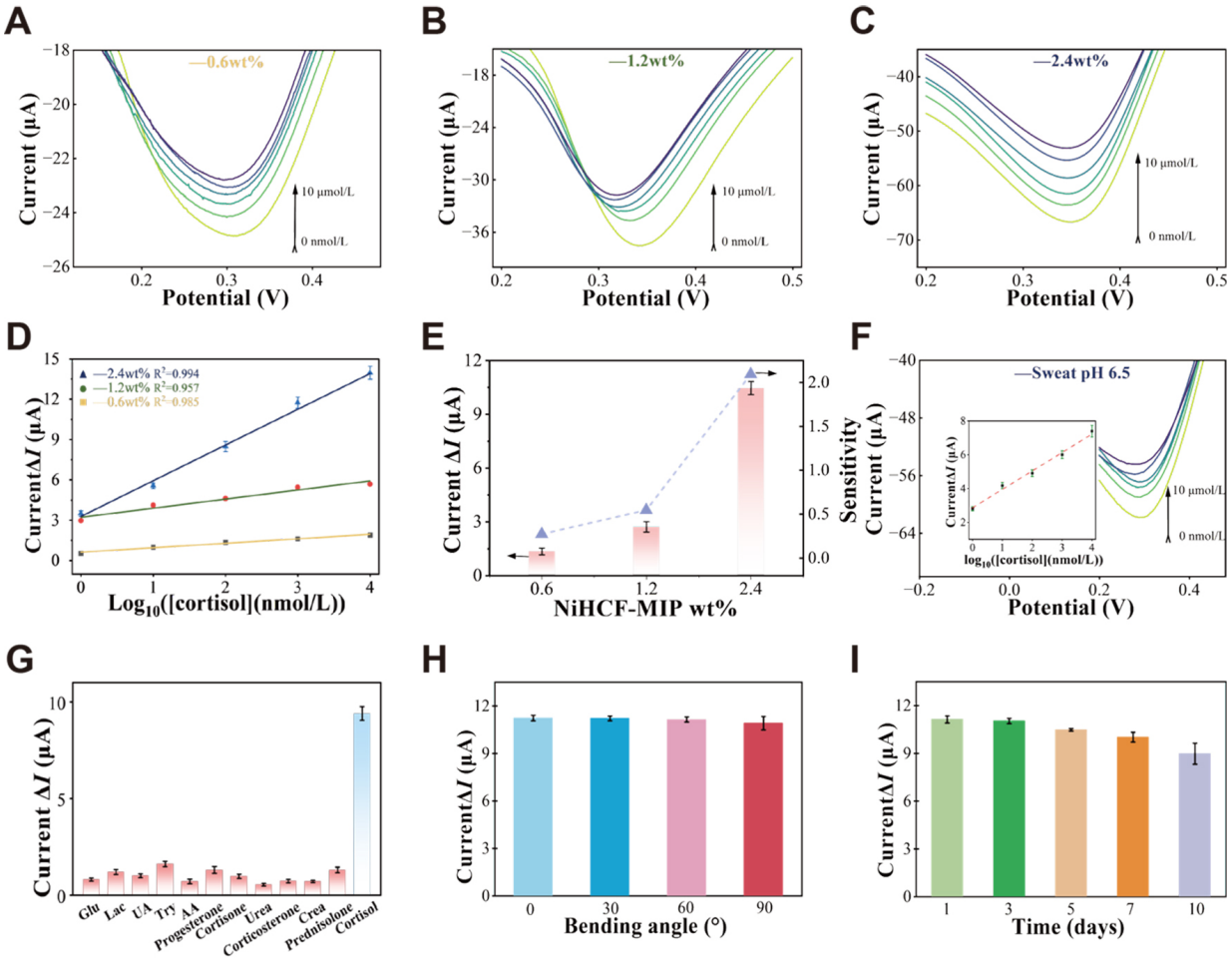

Figure 5. (A-C) LSV curves of the yarns prepared with different NiHCF-MIP amounts (0.6, 1.2, and 2.4 wt%) tested in blank and 1 nmol/L-10 μmol/L cortisol. Ag/AgCl as the reference electrode and Pt as the counter electrode; (D) Linear fitting plots (n = 3, signifying 3 independent sensors); (E) Summary and comparison of current difference (ΔI) and sensitivity (n = 3, signifying 3 independent sensors); (F) Calibration curve of the amperometric response versus cortisol concentration in artificial sweat, ranging from 1 nmol/L to 10 μmol/L. Inset: calibration plot with a linear fit (n = 3, signifying 3 independent sensors); (G) Selectivity of the yarns towards cortisol and other sweat secretions (n = 3, signifying 3 independent sensors); (H) LSV current response of the sensing fiber to a fixed cortisol concentration (1 μmol/L) under various mechanical deformations (e.g., bending at 0°, 30°, 60°, and 90°) (n = 3, signifying 3 independent sensors); (I) Long-term stability assessment of the fiber sensor for detecting a fixed cortisol concentration (1 μmol/L) (n = 3, signifying 3 independent sensors). Error bars represent the SD of the mean from three sensors in (D-I). LSV: Linear sweep voltammetry; NiHCF: nickel hexacyanoferrate; MIP: molecularly imprinted polymer; SD: standard deviation.

Table 1. Comparison of sensing properties with previous related reports

Sensing materials	Test methods	Sensitivity	LOD	Incubation time	Refs.
PB-MIP	CA	38.8 nA·dec^{-1}	0.9 nmol/L	120 s	[15]
AuNPs-MIP	SWV	2.061 μA·dec^{-1}	200 fmol/L	480 s	[35]
CNTfiber-PB-MIP	CA	48.7 μA·dec^{-1}	1 pmol/L	120 s	[19]
MXene/AuNPs-aptamer	DPV	0.389 μA·dec^{-1}	0.276 nmol/L	40 min	[36]
PB-MIP-PEDOT:PSS	LSV	2.549 μA·dec^{-1}	0.36 nmol/L	150 s	[37]
NiHCF-MIP	LSV	2.08 μA·dec^{-1}	0.4 nmol/L	120 s	This work

LOD: Limit of detection; PB: Prussian blue; MIP: molecularly imprinted polymer; CA: chronoamperometry; AuNPs: gold nanoparticles; SWV: square wave voltammetry; CNT: carbon nanotube; DPV: differential pulse voltammetry; PEDOT: poly(3,4-ethylenedioxythiophene); PSS: poly(styrenesulfonate); LSV: linear sweep voltammetry; NiHCF: nickel hexacyanoferrate.

cortisone, urea, corticosterone, creatinine (Crea), and prednisolone were sequentially added to PBS solutions, no significant signal changes were detected. Subsequently, upon the final addition of cortisol to a concentration of 10 μmol/L, a significant signal change was detected in the solution containing the mixture of interferents. This result demonstrates that the presence of these mixed interferents does not hinder the sensor's ability to detect the target analyte. The sensor demonstrates good selectivity toward cortisol, with negligible interference responses from common sweat constituents and structural analogs, indicating its promising potential for application in sweat-based real-time stress management[37].

Benefiting from the one-step electrospinning fabrication, the dual-function core-shell NiHCF-MIP nanocube probes are uniformly embedded within a three-dimensional nanofiber network, endowing the sensing fiber with enhanced mechanical stability and long-term durability. In terms of mechanical robustness, the current response of the sensing fiber was measured under bending angles of 0°, 30°, 60°, and 90°, during which the signal remained largely stable, with a relative standard deviation (RSD) of 1.3% [Figure 5H]. In parallel, the stability of the sensing fiber was further evaluated by monitoring its current response over a period of 10 days. The results indicated that the fiber retained 80% of its initial current response after this period, demonstrating excellent long-term durability [Figure 5I].

CONCLUSIONS

This study offers a synergistic framework that connects nanostructure engineering with scalable fabrication for high-performance wearable biosensing textiles. At the material level, the core-shell NiHCF-MIP NCs integrate specific molecular recognition and efficient electrochemical signal transduction into a single functional unit. At the device fabrication level, the one-step conjugate electrospinning technique enables continuous, high-yield production of functional coaxial yarns. This demonstrates a commercially viable pathway. The resulting sensing textiles combine excellent conductivity, mechanical flexibility, and rapid fluid uptake. These properties are essential for practical wearability. Thus, by integrating dual-function nanomaterials with continuous manufacturing, our proposed strategy creates a robust and scalable platform. This platform holds significant potential for advancing real-time, non-invasive personal health monitoring, particularly in applications such as continuous stress assessment and telehealth.

DECLARATIONS

Authors' contributions

Made substantial contributions to conception and design of the study: Cheng, J.; Zhao, Z.; Chen, W.
Performed data analysis and interpretation and wrote the manuscript: Cheng, J.; Hou, N.; Wang T.; Zhao, Z.
Performed data acquisition, as well as provided administrative, technical, and material support: Zhao Z.; Chen, W.

Availability of data and materials

The data that support the findings of this study are available from the corresponding author upon reasonable request.

AI and AI-assisted tools statement

Not applicable.

Financial support and sponsorship

The authors were supported by the HJ Program Research Funding Support from the National Natural Science Foundation of China (Grant No. 24210005-N); National Natural Science Foundation of China (Grant No. 21975214); Zhejiang Provincial Natural Science Foundation of China (Grant No. LQN26B030009); Science Foundation of Zhejiang Sci-Tech University (Grant Nos. 23212091-Y and 24212217-Y). The authors extend their gratitude to Mr. Deyo Chen (from Scientific Compass www.shiyanjia.com) for providing assistance with the TEM HRTEM image analysis.

Conflicts of interest

All authors declared that there are no conflicts of interest.

Ethical approval and consent to participate

Not applicable.

Consent for publication

Not applicable.

Supplementary Materials

Supplementary Materials

REFERENCES

1. De Kloet, E. R.; Joëls, M. The cortisol switch between vulnerability and resilience. *Mol. Psychiatry.* **2023**, *29*, 20-34. DOI PubMed
2. Stalder, T.; Oster, H.; Abelson, J. L.; Huthsteiner, K.; Klucken, T.; Clow, A. The cortisol awakening response: regulation and functional significance. *Endocr. Rev.* **2025**, *46*, 43-59. DOI PubMed
3. Kanaley, J. A.; Weltman, J. Y.; Pieper, K. S.; Weltman, A.; Hartman, M. L. Cortisol and growth hormone responses to exercise at different times of day. *J. Clin. Endocrinol. Metab.* **2001**, *86*, 2881-9. DOI PubMed
4. Van Smeden, L.; Saris, A.; Sergelen, K.; De Jong, A. M.; Yan, J.; Prins, M. W. J. Reversible immunosensor for the continuous monitoring of cortisol in blood plasma sampled with microdialysis. *ACS. Sens.* **2022**, *7*, 3041-8. DOI PubMed PMC
5. Bariya, M.; Nyein, H. Y. Y.; Javey, A. Wearable sweat sensors. *Nat. Electron.* **2018**, *1*, 160-71. DOI
6. Childs, A.; Mayol, B.; Lasalde-ramírez, J. A.; Song, Y.; Sempionatto, J. R.; Gao, W. Diving into sweat: advances, challenges, and future directions in wearable sweat sensing. *ACS. Nano.* **2024**, *18*, 24605-16. DOI PubMed PMC
7. Karuppaiah, G.; Lee, M.; Bhansali, S.; Manickam, P. Electrochemical sensors for cortisol detection: principles, designs, fabrication, and characterisation. *Biosens. Bioelectron.* **2023**, *239*, 115600. DOI PubMed
8. Tu, J.; Yeom, J.; Ulloa, J. C.; et al. Stressomic: a wearable microfluidic biosensor for dynamic profiling of multiple stress hormones in sweat. *Sci. Adv.* **2025**, *11*, eadx6491. DOI PubMed PMC
9. Wang, L.; Pagett, M.; Zhang, W. Molecularly imprinted polymer (MIP) based electrochemical sensors and their recent advances in health applications. *Sens. Actuators. Rep.* **2023**, *5*, 100153. DOI
10. Beyazit, S.; Tse Sum Bui, B.; Haupt, K.; Gonzato, C. Molecularly imprinted polymer nanomaterials and nanocomposites by controlled/living radical polymerization. *Prog. Polym. Sci.* **2016**, *62*, 1-21. DOI
11. Wu, S.; Zhang, Y.; Jia, X.; et al. Molecularly imprinted electrochemical sensor for ultrasensitive determination of chloramphenicol in milk and egg samples. *Food. Chem.* **2025**, *489*, 145024. DOI PubMed
12. Jiang, Y.; Yang, Y.; Shen, L.; Ma, J.; Ma, H.; Zhu, N. Recent advances of prussian blue-based wearable biosensors for healthcare. *Anal. Chem.* **2021**, *94*, 297-311. DOI PubMed
13. Wang, M.; Ye, C.; Yang, Y.; et al. Printable molecule-selective core-shell nanoparticles for wearable and implantable sensing. *Nat. Mater.* **2025**, *24*, 589-98. DOI PubMed PMC
14. Zhao, Z.; Hou, N.; Hong, Z.; Ming, S.; Lu, J.; Chen, W. Kinetic insights for high-rate and low-temperature ammonium-ion batteries/supercapacitors. *Energy. Storage. Mater.* **2025**, *81*, 104539. DOI
15. Tang, W.; Yin, L.; Sempionatto, J. R.; Moon, J. M.; Teymourian, H.; Wang, J. Touch-based stressless cortisol sensing. *Adv. Mater.* **2021**, *33*, 2008465.
16. Kim, H. H.; Kim, K.; Yang, J.; Choi, M. K. High-resolution intaglio transfer printing of silver nanowires for wearable electrophysiological sensors. *Adv. Mater. Technol.* **2023**, *9*, 2301262.
17. Deng, K.; Tang, Y.; Xiao, Y.; et al. A biodegradable, flexible photonic patch for *in vivo* phototherapy. *Nat. Commun.* **2023**, *14*, 3069.
18. Wang, L.; Wang, L.; Zhang, Y.; et al. Weaving sensing fibers into electrochemical fabric for real-time health monitoring. *Adv. Funct. Mater.* **2018**, *28*, 1804456. DOI
19. Hu, X.; Chen, Y.; Wang, X.; et al. Wearable and regenerable electrochemical fabric sensing system based on molecularly imprinted polymers for real-time stress management. *Adv. Funct. Mater.* **2024**, *34*, 2312897. DOI
20. Ma, X.; Wu, X.; Luo, W.; Liu, Z.; Wang, F.; Yu, H. Large-scale wearable textile-based sweat sensor with high sensitivity, rapid response, and stable electrochemical performance. *ACS. Appl. Mater. Interfaces.* **2024**, *16*, 18202-12. DOI PubMed

21. Wang, C.; Wang, W.; Qi, H.; et al. Electrospinning and electrospun nanofibers: From academic research to industrial production. *Prog. Mater. Sci.* **2025**, *154*, 101494. DOI
22. Cho, Y.; Baek, J. W.; Sagong, M.; Ahn, S.; Nam, J. S.; Kim, I. D. Electrospinning and nanofiber technology: fundamentals, innovations, and applications. *Adv. Mater.* **2025**, *37*, 2500162. DOI PubMed PMC
23. Lushaj, E.; Bordin, M.; Akbar, K.; et al. Highly efficient solar-light-driven photodegradation of metronidazole by nickel hexacyanoferrate nanocubes showing enhanced catalytic performances (Small Methods 2/2025). *Small. Methods.* **2025**, *9*, 2570012. DOI
24. Carter, S.; Rimmer, S. Surface molecularly imprinted polymer core-shell particles. *Adv. Funct. Mater.* **2004**, *14*, 553-61. DOI
25. Tang, J.; Wu, Y.; Ma, S.; Yan, T.; Pan, Z. Flexible strain sensor based on CNT/TPU composite nanofiber yarn for smart sports bandage. *Compos. Part. B. Eng.* **2022**, *232*, 109605. DOI
26. Piras, A.; Ehlert, C.; Gryn'ova, G. Sensing and sensitivity: computational chemistry of graphene-based sensors. *WIREs. Comput. Mol. Sci.* **2021**, *11*, e1526. DOI
27. Van Der Bent, J. F.; Puik, E. C. N.; Tong, H. D.; Van Rijn, C. J. M. Improving the limits of detection in potentiometric sensors. *Meas. Sci. Technol.* **2015**, *26*, 125104. DOI
28. Sapurina, I.; Bubulinca, C.; Trchová, M.; Prokeš, J.; Stejskal, J. Conducting polypyrrole and polypyrrole/manganese dioxide composites prepared with a solid sacrificial oxidant of pyrrole. *Synth. Met.* **2021**, *278*, 116807. DOI
29. Ming, Z.; Zhao, X.; Qin, W.; Wang, Y.; Yin, S. Molecularly imprinted sensor base on CNFs/CNTs aerogel for cortisol detection. *Microchem. J.* **2025**, *213*, 113849. DOI
30. Farahani, F.; Fazlali, A.; Kazazi, M. Enhanced supercapacitive performance of NiHCF/GO hybrid electrode prepared by layer-by-layer chemical deposition method. *J. Alloys. Compd.* **2025**, *1022*, 179882. DOI
31. Zhao, W.; He, P.; Ling, K.; et al. Printed graphene/CNTs/TPU-fabric wearable strain sensor for healthcare monitoring. *Soft. Sci.* **2025**, 10. DOI
32. Ji, D.; Lin, Y.; Guo, X.; et al. Electrospinning of nanofibres. *Nat. Rev. Methods. Primers.* **2024**, *4*, 1. DOI
33. Belbruno, J. J. Molecularly imprinted polymers. *Chem. Rev.* **2018**, *119*, 94-119. DOI PubMed
34. Sheng, F.; Zhao, C.; Zhang, B.; Tan, Y.; Dong, K. Flourishing electronic textiles towards pervasive, personalized and intelligent healthcare. *Soft. Sci.* **2024**, *4*, 2. DOI
35. Yeasmin, S.; Wu, B.; Liu, Y.; Ullah, A.; Cheng, L. Nano gold-doped molecularly imprinted electrochemical sensor for rapid and ultrasensitive cortisol detection. *Biosens. Bioelectron.* **2022**, *206*, 114142. DOI PubMed PMC
36. Tu, W.; Sun, M.; Lu, T.; et al. Wearable electrochemical aptasensor based on MXene@gold nanoparticles for non-invasive sweat cortisol detection. *Biosens. Bioelectron.* **2025**, *287*, 117736. DOI PubMed
37. Liu, Y.; Su, X.; Fan, P.; Liu, X.; Pan, Y.; Ping, J. Computationally-assisted wearable system for continuous cortisol monitoring. *Sci. Bull.* **2025**, *70*, 2004-13. DOI PubMed